American Diabetes Association. Cure • Care • Commitment
diabetes
A JOURNAL OF THE AMERICAN DIABETES ASSOCIATION

HDLs protect pancreatic beta cells against ER stress by restoring protein folding and trafficking

Journal:	*Diabetes*
Manuscript ID:	DB11-1221.R1
Manuscript Type:	Original Article
Date Submitted by the Author:	n/a
Complete List of Authors:	Petremand, Jannick; Lausanne University, Department of Physiology Puyal, Julien; Lausanne University, Department of Cell Biology and Morphology Chatton, Jean-Yves; Lausanne University, Department of Cell Biology and Morphology Duprez, Jessica; Université catholique de Louvain, Institute of experimental and clinical research Allagnat, Florent; Lausanne University Hospital, Frias, Miguel; University of Geneva, James, Richard; University of Geneva, Waeber, Gérard; Centre Hospitalier Universitaire Vaudois (CHUV), Jonas, Jean-Christophe; Université catholique de Louvain, Institute of experimental and clinical research Widmann, Christian; University of Lausanne, Department of Physiology
Key Words:	HDL, Stress, Endoplasmic Reticulum

HDLs protect pancreatic beta cells against ER stress by restoring protein folding and trafficking

Jannick Pétremand[1], Julien Puyal[2], Jean-Yves Chatton[2], Jessica Duprez[4], Florent Allagnat[3], Miguel Frias[5], Richard W. James[5], Gérard Waeber[3], Jean-Christophe Jonas[4], Christian Widmann[1]

[1] Department of Physiology and [2]Department of Cellular Biology and Morphology, University of Lausanne, Switzerland; [3]Department of Internal Medicine, Lausanne University Hospital, Lausanne, Switzerland; [4]Université Catholique de Louvain, Institute of experimental and clinical research, Pole of endocrinology, diabetes and nutrition, Brussels, Belgium; and [5]Lipoprotein Laboratory, Department of Internal Medicine, Faculty of Medicine, University of Geneva, Switzerland

Word count: 4462; Number of Tables: 0; Number of Figures:7

Running title: HDL-mediated ER functionality maintenance

Correspondence to Christian Widmann, Department of Physiology, Bugnon 7, 1005 Lausanne, Switzerland, Phone: +41 21 692 5123, Fax: +41 21 692 5505, E-mail: Christian.Widmann@unil.ch.

Abstract (145 words)

ER homeostasis alteration contributes to pancreatic beta cell dysfunction and death and favors the development of diabetes. In this study, we demonstrate that HDLs protect beta cells against ER stress induced by thapsigargin, cyclopiazonic acid, palmitate, insulin over-expression, and high glucose concentrations. ER stress marker induction and ER morphology disruption mediated by these stimuli were inhibited by HDLs. Using a temperature-sensitive viral glycoprotein folding mutant we show that HDLs correct impaired protein trafficking and folding induced by thapsigargin and palmitate. The ability of HDLs to protect beta cells against ER stress was inhibited by brefeldin A, an ER to Golgi trafficking blocker. These results indicate that HDLs restore ER homeostasis in response to ER stress, which is required for their ability to promote beta cell survival. This study identifies a cellular mechanism mediating the beneficial effect of HDLs on beta cells against ER stress-inducing factors.

Introduction

Pancreatic beta cells have a highly developed ER that reflects their physiological function as insulin-secreting cells. There is ample evidence indicating that alterations in ER homeostasis in beta cells affect their physiological function, increase their susceptibility to apoptosis, and contribute to the development of diabetes (1;2). Conversely, several of the factors that are involved in beta cell failure, including free fatty acids (FFAs), high glucose concentrations, and sustained insulin secretion, are known to induce ER stress in these cells (2-5). In response to ER stress, the protein chaperone BiP (immunoglobulin heavy chain-binding protein) dissociates from the ER transmembrane proteins ATF6 (activating transcription factor 6), IRE1α (inositol requiring 1 alpha) and PERK (protein kinase RNA-like endoplasmic reticulum kinase), allowing BiP to bind to unfolded or misfolded proteins to assist in their (re)folding. Dissociation from BiP also leads to IRE1α and PERK stimulation and ATF6 that is no longer bound to BiP translocates to the Golgi where it is cleaved and activated. The ensuing signaling events turn on UPR genes that encode, on one hand, proteins favoring the export and degradation of misfolded proteins and, on the other hand, proteins chaperones, including BiP, to increase the folding capacity of the ER. However, if ER stress is too strong and sustained, the transcription factor CHOP (C/EBP homologous protein-10) is expressed, leading to apoptosis by decreasing the expression of the anti-apoptotic Bcl-2 protein and by turning on the expression of apoptotic inducers such as death receptor 5 and Bim (6). In mice, genetic deletion of apoptotic mediators of the ER stress response (e.g. CHOP) can delay the development of diabetes (7). In humans, ER stress markers are associated with diabetes (8-10).

HDLs have crucial functions in cholesterol and lipid transport in the blood (11). In addition, HDLs exert multiple beneficial actions on cells by inducing anti-oxidative, anti-inflammatory and anti-apoptotic responses (12). Reduced levels of HDLs or HDL dysfunctions could therefore represent situations where the protective defense of an organism against metabolic stress is compromised. This is consistent with the fact that low HDL-cholesterol level is an independent risk factor for the development of type 2 diabetes (13;14). Reciprocally, most interventions that lead to increased HDL levels in humans are also known to reduce the risk of developing diabetes (15).

HDLs from diabetic patients display altered composition, notably higher triglyceride content and reduced cholesterol esters (16) and they are also more oxidized than HDLs from control subjects (17).

HDL modifications can alter their functionality. It has been shown for example that oxidized HDLs lose their ability to mediate cholesterol efflux (18).

The beneficial effect of HDLs against diabetes has been directly observed in humans where infusion of recombinant HDLs was found to improve beta cell function (19). This is again in line with the idea that HDLs have a positive effect on beta cell function and survival. Additionally, HDLs protect beta cells from cytokines and serum deprivation-induced apoptosis (20). Further, HDLs block oxidized LDL-induced cell death (21;22) and reduce apoptosis induced by high glucose concentrations and ER stress inducers (23;24). HDLs have also been reported to favor insulin secretion *in vitro* (25). However, the mechanisms underlying the beneficial effects of HDLs on beta cells remain largely unknown.

Characterizing how HDLs protect beta cells from ER stress is important in the context of the known anti-diabetogenic function of HDLs and their capacity to inhibit beta cell apoptosis. In this study, we provide evidence that HDLs protect beta cells against ER stress-inducing stimuli by improving protein folding and trafficking in the ER.

Research Design and Methods

Western blot analysis, cell transfection, apoptosis determination, immunocytochemistry, RNA extraction, reverse transcription, quantitative PCR, lentivirus preparation, ^{35}S-methionine incorporation, and nuclear extract preparation were performed as described (23;26). TUNEL assay on rat islets was performed as described earlier (5).

Antibodies

Antibodies recognizing CHOP and BiP were from Santa Cruz (catalog n°7351 and 13968, respectively). Antibodies specific for actin, caspase-3, phospho JNK, total JNK and phospho-PERK were from Cell Signaling (catalog n° 4968, 9661, 3179, 9252, 9251, respectively). 1E9 [called I14 in (27)] monoclonal antibody recognizing the correctly folded form of VSVG, 17-2-21-4 monoclonal antibody recognizing the VSVG protein exoplasmic domain and mouse IgG1κ monoclonal antibody specific for GM130 (Golgi matrix protein of 130 kDa) (BD Biosciences, catalog n°610822) were used for immunocytochemistry.

Primers

18S sense (5'-GCAATTATTCCCCATGAACG-3'), antisense (5'- GGCCTCACTAAACCATCCAA-3'). CHOP sense (5'- TTCACTACTCTTGACCCTGCGTC-3'), antisense (5'-CACTGACCACTCTGTTTCCGTTTC-3'), spliced XBP1 sense (GAGTCCGCAGCAGGTG), antisense (GTGTCAGAGTCCATGGGA), total XBP1 sense (AAGAACACGCTTGGGAATGG), antisense (ACTCCCCTTGGCCTCCAC).

Cells and cell culture

The MIN6B1 mouse insulinoma cell line (28) (referred here as MIN6) was cultured as described previously (23). Human islets were provided through the ECIT Islet for Basic Research program (JDRF award 31-2008-413). Islets were obtained from 4 different donors (see Supplemental Table 1 for the clinical characteristics of the donors). They were cultured in CMRL-1066 (GIBCO, catalog n°21530) medium containing 5 mM glucose, 100 units/ml penicillin, 100 mg/ml streptomycin and 10% FCS. Islets were trypsinized with trypsin-EDTA 0.5x for 6 minutes with pipetting every minute and then plated at a density of 150'000 cells per well (24-well plates). The following day, islets were treated as

indicated in the figures. Male Wistar rat islet isolation was performed as described earlier (5). All animal experimentations were approved by the local Institutional Committee on Animal Experimentation of the Faculty of Medicine of the Université catholique de Louvain (Project UCL/MD/2009/009).

Lipoprotein preparation and purification

Plasma lipoprotein fractions from human healthy donor serum were isolated on NaBr gradients by sequential ultracentrifugation, as described previously (29;30). The VLDL/IDL fraction (density 1.019) is isolated first, followed by the LDL fraction (density 1.063), and finally the HDL fraction (density 1.21). The fractions were dialyzed 48 hours against PBS, 100 µM EDTA and stored at 4°C. Before use, HDLs were dialyzed twice 24 hours against PBS. The medium used for dialysis (labeled "vehicle" in the figures) and HDLs were filtered through 0.22 µm filters. The cholesterol concentration of the fractions was measured by an enzymatic *in vitro* assay from Roche Applied Science (catalog n°2016630). The HDL and vehicle fractions were used within a 14 day-period. Experiments using HDLs were done with preparations from different donors or with mixed preparations and used at 1 mM cholesterol.

XBP1 mRNA splicing

Touchdown PCRs were performed using primers XBP1 sense (5'-AAACAGAGTAGCAGCGCAGACTGC-3'), antisense (5'-GGATCTCTAAAACTAGAGGCTTGGTG-3') and the Taq polymerase from Promega. PCR products were loaded on a 4% agarose gel and run for about 6 hours to discriminate the 26 nucleotides difference between the expected spliced and unspliced forms (600 bp). For rat islets, XBP1 mRNA splicing was measured as described earlier (5). In Figure 2A (middle panel) and in Figure 4B, qPCR was performed using previously described primers (31).

Plasmids

Plasmids mIns2-GFP (#688) and mIns2(C96Y)-GFP (#689), corresponding to pEGFP-Ins2-WT and pEGFP-Ins2-C96Y were described in reference (7), and were sub-cloned into the TRIP-PGK-ATGm-MCS-WHV* lentiviral vector (#349) generating plasmids mIns2-GFP.lti (#751) and mIns2(C96Y)-GFP.lti (#752). Plasmid pEGFP-VSVG (#729), obtained from Addgene, was sub-cloned into TRIP-PGK-ATGm-MCS-WHV* generating plasmid tsVSVG-GFP.lti (#730).

siRNA

siRNA, ordered from Microsynth (Balgach, Switzerland) sequences were the following siSRB1: 5' AGG UCA ACA UCA CCU UCA ATT 3', siGFP 5' GAC GUA AAC GGC CAC AAG UUG 3'.

Folding assay

MIN6 cells were plated on coverlips and infected with 2.5 ml of a temperature-sensitive (ts) vesicular stomatatis virus glycoprotein (VSVG)-GFP encoding lentivirus. Two days later, the cells were treated as mentioned in the figure legends. Cells were then fixed and cells on coverslips were subjected to immunocytochemistry labeling to detect correctly folded VSVG. At 32°C, the ts VSVG-GFP is synthesized on the ER and transits through the Golgi before reaching the plasma membrane. At the restrictive 40°C temperature, this protein is misfolded and accumulates in the ER. In neither case, does the protein accumulate in the cytoplasm (32).

Electron microscopy

MIN6 cells were plated in poly-L-lysine (0.01%, Sigma, catalog n°P4832)-coated glass slides (LabTek Chamber Slides, catalog n°177399) at a density of 110'000 cells per slide (area = 1.8 cm2), cultured for 3 days, and finally treated as indicated in the figures. Cells were then fixed 2 hours in 2.5% glutaraldehyde (Electron Microscopy Sciences, catalog n°16220) dissolved in 0.1 M phosphate buffer (PB), pH 7.4. After 3 washes in PB, MIN6 cells were post-fixed for 1 hour in 1% osmium tetroxide (Electron Microscopy Sciences, catalog n°19150) in PB, and then stained with ethanol 70% containing 1% uranyl acetate (Sigma, catalog n°73943) for 20 minutes. MIN6 cells were dehydrated in graded alcohol series and embedded in Epon (Electron Microscopy Sciences, catalog n°13940). Ultrathin sections (with silver to gray interference) were cut with a diamond knife (Diatome), mounted on Formvar-coated single slot grids and then counterstained with 3% uranyl acetate for 10 minutes and then with lead citrate (0.2%, Sigma, catalog n°15326) for 10 minutes. Sections were visualized using a Philips CM100 transmission electron microscope.

Palmitate preparation

HEPES-buffered Krebs Ringer (KRBH) solution (120 mM NaCl, 4 mM KH_2PO_4, 20 mM Hepes, 2 mM $MgCl_2$, 1 mM $CaCl_2$, 5 mM $NaHCO_3$) was equilibrated in a cell culture incubator at 37°C, 5% CO_2 for 1 hour. The pH was then adjusted to 7.4 and free fatty acid BSA (Sigma; catalog n°A60003) was

dissolved to a 5% concentration. The solution was then filtrated. Palmitate sodium salt was finally dissolved in the KRBH-BSA solution to a 6.7 mM concentration.

Oxidized HDL

HDLs were oxidised at 37°C using 2,2'-azobis (2-amidinopropane) hydrochloride (AAPH) as described previously (33). The reaction was stopped by placing the mixture on ice and AAPH removed by dialysis. Lipoperoxide concentrations were determined using the Fox assay (34).

Data presentation and statistics

Results are expressed as the mean ± 95% confidence intervals (CI) of three independent experiments unless otherwise stated. The statistical tests used were paired t-test with Bonferroni corrections in the case of results derived from independent experiments performed in monoplicate (Figure 1D; Figures 2 A-B, right panels; and Figure 5) and one way ANOVAs for all other cases.

Results

HDLs protect beta cells against ER stressor-induced apoptosis

To determine if HDLs antagonize the negative effects of patho-physiological ER stressors or ER stress-inducing drugs on beta cells, we first used thapsigargin (TG) on mouse insulinoma cells, as well as on human and rat islets. TG is a SERCA (sarco/endoplasmic reticulum Ca^{2+}-ATPase) inhibitor that induces ER calcium depletion and ER stress (35). Apoptosis induced by TG in primary human islet cells was decreased by HDLs (Figure 1A). Similarly, primary rat beta cells were protected by HDLs against TG-induced apoptosis (Figure 1B). In the MIN6 mouse insulinoma cell line, HDLs very efficiently inhibited TG-induced apoptosis as indicated by a reduction in the number of cells with pycnotic nucleus and by a decrease in caspase-3 activation (Figure 1C). HDLs also protected MIN6 cells against cyclopiazonic acid (CPA)-induced death, another SERCA inhibitor (Supplemental Figure 1). Free fatty acids contribute to the development of type 2 diabetes by inducing ER stress, beta-cell dysfunction and apoptosis (36). Palmitate-induced apoptosis was significantly reduced by HDLs (Figure 1D). Hyperglycemia, observed in diabetic patient, is another factor suggested to induce ER stress in pancreatic islets (37). One week exposure of rat islets to 30 mM glucose almost quadrupled the rate of apoptosis in insulin-expressing cells (Figure 1 E-F). This was fully prevented by HDLs (Figure 1 E-F). Altogether, these results indicate that HDLs protect beta cells against a broad range of patho-physiological ER stressors.

In endothelial cells, HDLs activate the anti-apoptotic Akt kinase (38) and this presumably requires binding of HDLs to the scavenger receptor class B, type I (SR-BI) (39;40). In beta cells, SR-BI does not appear to be involved in HDL-induced suppression of IL1β-mediated apoptosis (24). Whether SR-BI is involved or not in beta cell protection may depend on the pro-apoptotic stimulus however. We therefore tested whether this receptor could mediate the protective effect of HDLs against ER stress. MIN6 cells were transfected with siRNA duplexes directed at the SR-BI mRNA. This led to a ~80% reduction in SR-BI protein expression levels (Supplemental Figure 2C). In these conditions, HDLs were still able to protect beta-cells against both TG and palmitate-induced apoptosis (Supplemental Figure 2 A and B). This suggests that SR-BI is dispensable for HDL-mediated beta cell protection.

Specificity of the HDL-induced protection against TG-induced beta cell apoptosis

TG is a lipophilic compound that could potentially bind to HDLs, preventing it from inhibiting SERCA. To determine whether HDLs could affect the SERCA inhibitory activity of TG, cytosolic calcium concentration was monitored by Fura-2 calcium imaging. Supplemental Figure 3 shows that TG, as expected from its ability to induce ER calcium depletion, stimulated an increase in cytoplasmic calcium. HDLs did not affect this response, indicating that they do not prevent the inhibitory activity of TG on SERCA. We next assessed the specificity of the protective response induced by HDLs in beta cells by testing the capacity of another lipoprotein, the low density lipoprotein (LDL), to prevent TG-induced MIN6 cells apoptosis. LDLs are not toxic for beta cells unless oxidized (22) (compare also the first and third bar in Supplemental Figure 4). LDLs were unable to protect MIN6 cells from death induced by TG (Supplemental Figure 4). This demonstrates that the ability of HDLs to protect beta cells from ER stress is specific for this lipoprotein particle and that it is not a general property of lipoproteins.

To further characterize the protective effects of HDLs, MIN6 cells were subjected to different TG incubation protocols prior to HDL addition. Supplemental Figure 5A (grey bars) shows that HDLs added 10 minutes after TG still prevented apoptosis of MIN6 cells, indicating that HDLs protect beta cells when TG had already started the depletion in ER calcium stores (that occurs within less than a minute; see Supplemental Figure 3). However, continuous TG exposure is required to induce efficient apoptosis of MIN6 cells as washing TG after a ten-minute incubation period greatly reduced the extent of cell death (Supplemental Figure 5A, black bars). Supplemental Figure 5B shows indeed that TG has to be present for several hours to induce a clear increase in MIN6 cell death. The same experiment as described in Supplemental Figure 5A was then performed but with longer incubation times with TG (Supplemental Figure 5C). In each case, HDLs significantly reduced the extent of apoptosis after removal of TG. Finally, in conditions where TG was added at the beginning of the experiment and was not washed away, addition of HDLs at later times still protected beta cells (Supplemental Figure 5D). The degree of protection was still about 70% when HDLs were added 12 hours after the addition of TG. Altogether these experiments indicate that HDLs can reverse the pro-apoptotic effects of TG, which is consistent with their ability to reverse the ER morphological alterations induced by TG (see Figure 3 below).

HDLs prevent ER stress signaling

TG and palmitate induced ER stress in MIN6 cells and primary rat islet cells as assessed by their ability to increase XBP1 mRNA splicing (Figure 2A), CHOP mRNA and nuclear protein levels (Figure 2B and Figure 2C, respectively), BiP protein levels (Figure 2D), and phosphorylation of PERK (Figure 2E) and JNK (Figure 2F). Induction of all these ER stress markers was significantly inhibited by HDLs. Therefore, the ability of HDLs to prevent beta cell death induced by TG and palmitate correlates with their capacity to dampen ER stress signaling.

HDLs reverse TG-induced ER morphology disruption

As previously reported (41), TG induced extensive dilation of the ER after a 6 hour-incubation period (compare the first and second rows in Figure 3A). This was prevented by HDLs (fourth row in Figure 3A). A 24 hour-treatment with TG, in addition to inducing ER swelling, led to the appearance of apoptotic features such as chromatin condensation and pycnosis (Figure 3B). When HDLs were added 6 hours after TG - i.e. at a time when ER was extensively dilated (see Figure 3A) - and incubated for an additional 18 hour-period in the presence of TG, ER morphology greatly recovered and the signs of apoptosis disappeared. Palmitate also induced ER dilation, although to a lesser extent than TG, but importantly this was efficiently prevented by HDLs (Figure 3C). These results indicate that HDLs not only prevent ER morphology disruption brought about by ER stress, but also allow cells with disrupted ER to recover a normal morphology even in the continuous presence of an ER stressor.

HDLs improve protein folding and export capacity of the ER

The ability of HDLs to inhibit apoptosis induced by ER stressors could result from an augmented capacity of the ER to fold proteins and favor their export or from an increased capacity to tolerate a given ER stress. As a first approach to distinguish between these two possibilities, we over-expressed GFP fusion proteins with wild-type insulin-2 and a mutant form of insulin-2, found in the Akita mouse, that cannot fold properly due to a cysteine to tyrosine substitution at position 96. This mutation prevents the formation of a disulfide bridge required for insulin maturation (42). Thus the (re)folding mechanisms of the cell cannot correct this altered conformation, leading to sustain ER stress and apoptosis (7), unless downstream pro-apoptotic effectors, such as CHOP, are inactivated (7). Expression of the insulin-GFP fusion protein in MIN6 cells following lentiviral infection led to a ~60% increase in total insulin content (i.e. endogenous insulin + insulin-GFP; Supplemental Table 2) and this induced a mild but significant apoptotic response (Figure 4A). Expression of the insulin-GFP

constructs by transfection similarly induced apoptosis (Supplemental Figure 6). In each case, the apoptotic response mediated by insulin over-expression was blocked by HDLs. In contrast, apoptosis induced by expression of the insulin C96Y-GFP mutant in MIN6 cells was not antagonized by HDLs (Figure 4A and Supplemental Figure 6). Paralleling these responses, XBP-1 mRNA splicing was augmented by both wild-type and mutant insulin, but HDLs only inhibited the splicing of XBP-1 mRNA induced by wild-type insulin (Figure 4B). This indicates that over-expression of the C96Y insulin mutant exerts a stress on the ER that may be more severe (or of a different nature) than the one induced by wild-type insulin over-expression, a stress that cannot be tuned down by HDLs. The C96Y insulin mutant appears indeed to induce a stronger burden on the ER than wild-type insulin because it significantly increased CHOP expression while wild-type insulin did not (Figure 4C). The increased CHOP expression following over-expression of the insulin C96Y mutant was not antagonized by HDLs (Figure 4C). One interpretation of the above results is that HDLs do not protect beta cells experiencing an ER stress response that cannot be alleviated such as when cells express an insulin mutant that cannot fold properly.

HDLs may protect beta cells against ER stress by increasing the functionality of the ER eventually dampening the initial ER stress. This is consistent with the ability of HDLs to lower the expression of ER stress markers induced by TG and palmitate (see Figure 2). To directly assess the capacity of HDLs to favor protein folding and trafficking, we took advantage of a temperature-sensitive mutant of a vesicular stomatitis virus glycoprotein (VSVG) fused to GFP (32). This mutant cannot fold correctly at 40°C and is therefore retained in the ER. However, at the permissive temperature (32°C), it adopts a correctly folded conformation, and can then traffic from the ER to the Golgi and finally to the cell surface. As expected, cells cultured at 32°C expressed the correctly folded VSVG-GFP fusion protein as determined by staining with a conformation-specific anti-VSVG antibody (Cy3-positive cells in Supplemental Figure 7). At 40°C, no cells expressed the correctly folded VSVG protein whether HDLs were present or not (Supplemental Figure 7). HDLs were not able to increase the VSVG folding capacity of the cells at 39°C, a temperature that allowed partial folding of VSVG (Supplemental Figure 7). Possibly, VSVG misfolding induced by high temperatures is intrinsically irreversible, akin to the misfolding of the C96Y insulin mutant.

To determine whether HDLs can favor protein folding and trafficking in the presence of an ER stressor, we evaluated the influence of HDLs on VSVG folding and trafficking in conditions where HDLs can

inhibit apoptosis. MIN6 cells were incubated or not with TG in the presence or absence of HDLs (Figure 5). A five hour incubation at 40°C led to accumulation of misfolded VSVG in the ER (Figure 5A, left panel). Releasing this block by placing the cells at 32°C allowed VSVG to be correctly folded (Figure 5A, right panel). This was prevented by TG indicating that this SERCA inhibitor impairs protein folding. HDLs, however, restored the capacity of the cells to correctly fold the VSVG protein in the presence of TG (Figure 5A-B). Protein trafficking was assessed by monitoring the appearance of VSVG at the cell surface following the release of the cells from the 40°C block. Figure 5C shows that TG did not allow cell surface appearance of VSVG (Figure 5C, right panel). This was reversed by HDLs (Figure 5C-D). HDLs can therefore inhibit the capacity of TG to hamper the correct folding of VSVG and its trafficking from the ER to the surface of the cells. We also noted that TG decreased the expression of the VSVG-GFP fusion protein (Figure 5C-E) indicating that this ER stressor also perturbs protein synthesis possibly as a result of ER homeostasis alteration. This again was not occurring in the presence of HDLs (Figure 5C-E).

The causality between the ability of HDLs to efficiently protect beta cells against ER stress and their capacity to improve the trafficking of proteins was investigated using brefeldin A (BFA). This compound is able to inhibit the trafficking of protein from the ER to the Golgi (43). Hence as expected, BFA blocked the translocation of VSVG from the ER to the Golgi (Figure 5F). Figure 5G shows that BFA prevented HDLs from inhibiting TG-induced beta cell apoptosis. This indicates that the capacity of HDLs to promote protein trafficking in the presence of an ER stress is required for their anti-apoptotic ability.

We next analyzed the ability of HDLs to prevent ER protein export perturbation induced by palmitate. Palmitate was shown earlier to impair ER to Golgi trafficking (44). However, palmitate does not reduce VSVG folding (44). Thirty minutes following the release from the 40°C block, about 50% of the cells had the majority of their VSVG proteins move from the ER to the Golgi (Figure 6). ER export of VSVG was reduced by palmitate but this was antagonized by HDLs (Figure 6C). As previously reported, palmitate did not affect VSVG folding (Figure 6D). Interestingly, the presence of HDLs alone was able to slightly, but significantly, increase the number of correctly folded VSVG. This suggests that HDLs contribute to improve beta cell ER homeostasis by favoring both protein folding and trafficking.

HDL oxidation is one alteration that is thought to occur in diabetes or in the metabolic syndrome (45). Therefore, it was of interest to assess the capacity of oxidized HDLs to protect beta cells against ER stress-induced apoptosis. Figure 7 shows that, in contrast to native HDLs, oxidized HDLs were not able to antagonize TG-induced apoptosis of MIN6 cells.

Discussion

In the present study, HDLs were found to efficiently inhibit apoptosis induced by several ER stressors (Figure 1). This was observed both in insulinoma cells and in primary human and rat islet beta cells. This protection was associated with a diminished activation of ER stress markers including XBP1 mRNA splicing, CHOP induction (both at the RNA and protein level), BiP induction, PERK activation and JNK MAPK stimulation (Figure 2). A series of control experiments was performed to assess the possibility that HDLs could exert their protective action against the ER stressors (TG in particular) by merely sequestering them away from cells. This possibility could be excluded because of the following observations. HDLs did not prevent TG from inducing an increase in cytoplasmic calcium concentration following its inhibitory action on SERCA (Supplementary Figure 3). LDL, a similar amphipathic lipoprotein was unable to mimic the anti-apoptotic properties of HDLs (Supplementary Figure 4). Addition of HDLs several hours after TG still inhibited beta cell apoptosis (Supplementary Figure 4) and was able to restore a normal ER morphology (Figure 3). HDLs prevented beta cell apoptosis and ER stress marker induction in response to chemically unrelated substances and treatments (palmitate, CPA, TG, insulin over-expression) (Figures 1, 2, 4 and Supplemental Figure 1). Finally, if HDLs sequestered TG away from cells, they would be expected to always protect cells from TG-induced apoptosis. However, this is not the case as HDLs do in fact lose their capacity to inhibit TG-induced beta cell apoptosis in certain experimental conditions (e.g. when cell are treated with BFA; see Figure 5F-G).

HDLs are known to induce anti-apoptotic pathways in various cell types. This has been well studied in endothelial cells where HDLs stimulate the anti-apoptotic Akt kinase (38). EDG receptors and the scavenger receptor SR-B1 are likely to mediate HDL effects in these cells (39;40;46). In contrast, the signaling pathways mediating HDL-induced anti-apoptotic response in beta cells are not known. Further, SR-BI does not seem to be involved in HDL-mediated protection of IL1β-treated beta cells (24;47) or against TG- and palmitate-induced death (Supplementary Figure 2). The paucity of information on the signaling pathways that are involved in the protective function induced by HDLs in beta cells contrasts with the numerous data showing beneficial effects of HDLs against diabetes in rodents and humans.

Our data show that HDL-mediated beta cell protection correlates with ER morphology preservation, as well as maintenance of a functional protein folding in the ER and protein export from the ER. However when protein transport from the ER to the Golgi was inhibited with BFA, HDLs lost their protective effect (Figure 5F-G), indicating that the maintenance of a proper ER secretory capacity is required for HDL-induced inhibition of ER stressor-induced beta cell apoptosis. HDL-mediated protection of beta cells via improved protein folding and ER export is the first cellular mechanism to be identified explaining how HDLs protect beta cells against pro-diabetogenic factors such as FFAs, high glucose concentrations, and ER overload. Improved functionality of the ER could also participate in the known capacity of HDLs to ameliorate the insulin secretory capacity of beta cell (19;25). Our data suggest that improved ER functionality is an underlying mechanism counteracting the development of diabetes during interventions to increase HDL levels in humans exposed to pro-diabetogenic factors. Our findings are in line with the notion that alleviating ER stress is a new avenue to treat diabetes (48). We have observed that oxidation of HDLs abrogates their ability to protect beta cells against ER stress-induced apoptosis (Figure 7). Therefore, one of the contributions to accelerated beta cell mass decrease in diabetic patients, who have increased levels of oxidized HDLs (45), may be an inefficient HDL-mediated protection of beta cells against ER stress. Hence, means of preserving HDLs integrity and functionality represent potential avenues of treatments against diabetes.

Acknowledgements

This study was supported by the Swiss National Science Foundation (to CW and GW), the Belgian National Fund for Scientific Research (to JCJ), and by a FRIA fellowship (Brussels, Belgium) to JD.

No potential conflicts of interest relevant to this article were reported.

Jannick P, GW, and CW designed the experiments. Jannick P and CW co-wrote the paper. Experiments on rat islets were performed by JCJ and JD. Electron microscopy was performed by Julien P. Fluorescence calcium imaging was performed by JYC. RF and RWJ performed the oxidation of HDLs. FA quantitated insulin. All other experiments were performed by Jannick P. All authors discussed the results and edited the paper. JP and CW are the guarantors of this article.

We thank Dr. Seiichi Oyadomari (University of Tokushima, Japan) for the kind gift of plasmids pEGFP-Ins2-WT and pEGFP-Ins2-C96Y. We are grateful to Dr. Douglas S. Lyles (Wake Forest University School of Medicine, North Carolina) and Dr. Jean Grünberg (University of Geneva, Switzerland) for providing us with aliquots of the antibody recognizing the folded form of VSVG and the antibody recognizing the ectopic part of VSVG, respectively. We thank Dr. Claudiane Guay and Dr. Romano Regazzi (University of Lausanne, Switzerland) for giving us palmitate aliquots. MIN6B1 cells (49) were provided by Dr. Philippe Halban (University of Geneva, Switzerland) with permission from Dr. Jun-ichi Miyazaki, University of Osaka who produced the maternal MIN6 cell line (28). We thank Dr. Francesca Amati (University of Lausanne, Switzerland) and Dr. Andrew Dwyer (Centre Hospitalier Universitaire Vaudois, Lausanne, Switzerland) for critical reading of the manuscript. We thank Jean Daraspe (University of Lausanne, Switzerland) for technical assistance and the Center of Electron Microscopy at the University of Lausanne for the use of their electron microscopes. We thank Mrs. Marie-Claude Brulhart (University of Geneva, Switzerland) for shipment of HDLs and performing the Fox assay.

Reference List

1. Eizirik,DL, Cnop,M: ER stress in pancreatic beta cells: the thin red line between adaptation and failure. *Sci Signal* 3:e7, 2010

2. Eizirik,DL, Cardozo,AK, Cnop,M: The role for endoplasmic reticulum stress in diabetes mellitus. *Endocr Rev* 29:42-61, 2008

3. Oyadomari,S, Araki,E, Mori,M: Endoplasmic reticulum stress-mediated apoptosis in pancreatic beta-cells. *Apoptosis* 7:335-345, 2002

4. Cnop,M, Welsh,N, Jonas,JC, Jorns,A, Lenzen,S, Eizirik,DL: Mechanisms of pancreatic β-cell death in type 1 and type 2 diabetes: many differences, few similarities. *Diabetes* 54 Suppl 2:S97-S107, 2005

5. Elouil,H, Bensellam,M, Guiot,Y, Vander,MD, Pascal,SM, Schuit,FC, Jonas,JC: Acute nutrient regulation of the unfolded protein response and integrated stress response in cultured rat pancreatic islets. *Diabetologia* 50:1442-1452, 2007

6. Ron,D, Walter,P: Signal integration in the endoplasmic reticulum unfolded protein response. *Nat Rev Mol Cell Biol* 8:519-529, 2007

7. Oyadomari,S, Koizumi,A, Takeda,K, Gotoh,T, Akira,S, Araki,E, Mori,M: Targeted disruption of the Chop gene delays endoplasmic reticulum stress-mediated diabetes. *J Clin Invest* 109:525-532, 2002

8. Huang,CJ, Lin,CY, Haataja,L, Gurlo,T, Butler,AE, Rizza,RA, Butler,PC: High expression rates of human islet amyloid polypeptide induce endoplasmic reticulum stress mediated beta-cell apoptosis, a characteristic of humans with type 2 but not type 1 diabetes. *Diabetes* 56:2016-2027, 2007

9. Laybutt,DR, Preston,AM, Akerfeldt,MC, Kench,JG, Busch,AK, Biankin,AV, Biden,TJ: Endoplasmic reticulum stress contributes to beta cell apoptosis in type 2 diabetes. *Diabetologia* 50:752-763, 2007

10. Marchetti,P, Bugliani,M, Lupi,R, Marselli,L, Masini,M, Boggi,U, Filipponi,F, Weir,GC, Eizirik,DL, Cnop,M: The endoplasmic reticulum in pancreatic beta cells of type 2 diabetes patients. *Diabetologia* 50:2486-2494, 2007

11. Eisenberg,S: High density lipoprotein metabolism. *J Lipid Res* 25:1017-1058, 1984

12. von Eckardstein,A, Hersberger,M, Rohrer,L: Current understanding of the metabolism and biological actions of HDL. *Curr Opin Clin Nutr Metab Care* 8:147-152, 2005

13. von Eckardstein,A, Schulte,H, Assmann,G: Risk for diabetes mellitus in middle-aged Caucasian male participants of the PROCAM study: implications for the definition of impaired fasting glucose by the American Diabetes Association. *J Clin Endocrinol Metab* 85:3101-3108, 2000

14. Montonen,J, Drogan,D, Joost,HG, Boeing,H, Fritsche,A, Schleicher,E, Schulze,MB, Pischon,T: Estimation of the contribution of biomarkers of different metabolic pathways to risk of type 2 diabetes. *Eur J Epidemiol* 26:29-38, 2011

15. Laaksonen,MA, Knekt,P, Rissanen,H, Harkanen,T, Virtala,E, Marniemi,J, Aromaa,A, Heliovaara,M, Reunanen,A: The relative importance of modifiable potential risk factors of type 2 diabetes: a meta-analysis of two cohorts. *Eur J Epidemiol* 25:115-124, 2010

16. Kruit,JK, Brunham,LR, Verchere,CB, Hayden,MR: HDL and LDL cholesterol significantly influence beta-cell function in type 2 diabetes mellitus. *Curr Opin Lipidol* 21:178-185, 2010

17. Ueda,M, Hayase,Y, Mashiba,S: Establishment and evaluation of 2 monoclonal antibodies against oxidized apolipoprotein A-I (apoA-I) and its application to determine blood oxidized apoA-I levels. *Clin Chim Acta* 378:105-111, 2007

18. Nagano,Y, Arai,H, Kita,T: High density lipoprotein loses its effect to stimulate efflux of cholesterol from foam cells after oxidative modification. *Proc Natl Acad Sci U S A* 88:6457-6461, 1991

19. Drew,BG, Duffy,SJ, Formosa,MF, Natoli,AK, Henstridge,DC, Penfold,SA, Thomas,WG, Mukhamedova,N, de Court, Forbes,JM, Yap,FY, Kaye,DM, van,HG, Febbraio,MA, Kemp,BE, Sviridov,D, Steinberg,GR, Kingwell,BA: High-density lipoprotein modulates glucose metabolism in patients with type 2 diabetes mellitus. *Circulation* 119:2103-2111, 2009

20. Roehrich,ME, Mooser,V, Lenain,V, Herz,J, Nimpf,J, Azhar,S, Bideau,M, Capponi,A, Nicod,P, Haefliger,JA, Waeber,G: Insulin-secreting β-cell dysfunction induced by human lipoproteins. *J Biol Chem* 278:18368-18375, 2003

21. Cnop,M, Hannaert,JC, Grupping,AY, Pipeleers,DG: Low density lipoprotein can cause death of islet beta-cells by its cellular uptake and oxidative modification. *Endocrinology* 143:3449-3453, 2002

22. Abderrahmani,A, Niederhauser,G, Favre,D, Abdelli,S, Ferdaoussi,M, Yang,JY, Regazzi,R, Widmann,C, Waeber,G: Human high-density lipoprotein particles prevent activation of the JNK pathway induced by human oxidised low-density lipoprotein particles in pancreatic β cells. *Diabetologia* 50:1304-1314, 2007

23. Petremand,J, Bulat,N, Butty,AC, Poussin,C, Rutti,S, Au,K, Ghosh,S, Mooser,V, Thorens,B, Yang,JY, Widmann,C, Waeber,G: Involvement of 4E-BP1 in the protection induced by HDLs on pancreatic beta cells. *Mol Endocrinol* 23:1572-1586, 2009

24. Rutti,S, Ehses,JA, Sibler,RA, Prazak,R, Rohrer,L, Georgopoulos,S, Meier,DT, Niclauss,N, Berney,T, Donath,MY, von Eckardstein,A: Low and high-density lipoproteins modulate function, apoptosis and proliferation of primary human and murine pancreatic beta cells. *Endocrinology* 150:4521-4530, 2009

25. Fryirs,MA, Barter,PJ, Appavoo,M, Tuch,BE, Tabet,F, Heather,AK, Rye,KA: Effects of high-density lipoproteins on pancreatic beta-cell insulin secretion. *Arterioscler Thromb Vasc Biol* 30:1642-1648, 2010

26. Bulat,N, Jaccard,E, Peltzer,N, Khalil,H, Yang,JY, Dubuis,G, Widmann,C: RasGAP-derived fragment N increases the resistance of beta cells towards apoptosis in NOD mice and delays the progression from mild to overt diabetes. *PLoS ONE* 6:e22609, 2011

27. Lefrancois,L, Lyles,DS: The interaction of antibody with the major surface glycoprotein of vesicular stomatitis virus. I. Analysis of neutralizing epitopes with monoclonal antibodies. *Virology* 121:157-167, 1982

28. Miyazaki,J, Araki,K, Yamato,E, Ikegami,H, Asano,T, Shibasaki,Y, Oka,Y, Yamamura,K: Establishment of a pancreatic beta cell line that retains glucose-inducible insulin secretion: special reference to expression of glucose transporter isoforms. *Endocrinology* 127:126-132, 1990

29. Havel,RJ, Eder,HA, Bragton,JH: The distribution and chemical composition of ultracentrifugally separated lipoproteins in human serum. *J Clin Invest* 34:1345-1353, 1955

30. James,RW, Pometta,D: Differences in lipoprotein subfraction composition and distribution between type I diabetic men and control subjects. *Diabetes* 39:1158-1164, 1990

31. Zhang,K, Kaufman,RJ: Identification and characterization of endoplasmic reticulum stress-induced apoptosis in vivo. *Methods Enzymol* 442:395-419, 2008

32. Presley,JF, Cole,NB, Schroer,TA, Hirschberg,K, Zaal,KJ, Lippincott-Schwartz,J: ER-to-Golgi transport visualized in living cells. *Nature* 389:81-85, 1997

33. Deakin,S, Moren,X, James,RW: HDL oxidation compromises its influence on paraoxonase-1 secretion and its capacity to modulate enzyme activity. *Arterioscler Thromb Vasc Biol* 27:1146-1152, 2007

34. Wolff,SP: Ferrous ion oxidation in the presence of the ferric ion indicator xylenol orange for the measure of hydroperoxydes: the FOX assay. *Methods Enzymol* 233:182-189, 1994

35. Sambrook,JF: The involvement of calcium in transport of secretory proteins from the endoplasmic reticulum. *Cell* 61:197-199, 1990

36. Petremand,J, Widmann,C: Genetics and molecular biology: fatty acids and endoplasmic reticulum stress. *Curr Opin Lipidol* 22:315-316, 2011

37. Weir,GC, Laybutt,DR, Kaneto,H, Bonner-Weir,S, Sharma,A: Beta-cell adaptation and decompensation during the progression of diabetes. *Diabetes* 50 Suppl 1:S154-S159, 2001

38. Nofer,JR, Levkau,B, Wolinska,I, Junker,R, Fobker,M, von Eckardstein,A, Seedorf,U, Assmann,G: Suppression of endothelial cell apoptosis by high density lipoproteins (HDL) and HDL-associated lysosphingolipids. *J Biol Chem* 276:34480-34485, 2001

39. Nofer,JR, van der,GM, Tolle,M, Wolinska,I, von Wnuck,LK, Baba,HA, Tietge,UJ, Godecke,A, Ishii,I, Kleuser,B, Schafers,M, Fobker,M, Zidek,W, Assmann,G, Chun,J, Levkau,B: HDL induces NO-dependent vasorelaxation via the lysophospholipid receptor S1P3. *J Clin Invest* 113:569-581, 2004

40. Kimura,T, Tomura,H, Sato,K, Ito,M, Matsuoka,I, Im,DS, Kuwabara,A, Mogi,C, Itoh,H, Kurose,H, Murakami,M, Okajima,F: Mechanism and role of high density lipoprotein-induced activation of AMP-activated protein kinase in endothelial cells. *J Biol Chem* 285:4387-4397, 2010

41. Yoshida,I, Monji,A, Tashiro,K, Nakamura,K, Inoue,R, Kanba,S: Depletion of intracellular Ca^{2+} store itself may be a major factor in thapsigargin-induced ER stress and apoptosis in PC12 cells. *Neurochem Int* 48:696-702, 2006

42. Wang,J, Takeuchi,T, Tanaka,S, Kubo,SK, Kayo,T, Lu,D, Takata,K, Koizumi,A, Izumi,T: A mutation in the insulin 2 gene induces diabetes with severe pancreatic beta-cell dysfunction in the Mody mouse. *J Clin Invest* 103:27-37, 1999

43. Donaldson,JG, Finazzi,D, Klausner,RD: Brefeldin A inhibits Golgi membrane-catalysed exchange of guanine nucleotide onto ARF protein. *Nature* 360:350-352, 1992

44. Preston,AM, Gurisik,E, Bartley,C, Laybutt,DR, Biden,TJ: Reduced endoplasmic reticulum (ER)-to-Golgi protein trafficking contributes to ER stress in lipotoxic mouse beta cells by promoting protein overload. *Diabetologia* 52:2369-2373, 2009

45. Pan,B, Ren,H, Ma,Y, Liu,D, Yu,B, Ji,L, Pan,L, Li,J, Yang,L, Lv,X, Shen,X, Chen,B, Zhang,Y, Willard,B, He,Y, Zheng,L: HDL of patients with type 2 diabetes mellitus elevates the capability of promoting migration and invasion of breast cancer cells. *Int J Cancer* 2011

46. Al-Jarallah,A, Trigatti,BL: A role for the scavenger receptor, class B type I in high density lipoprotein dependent activation of cellular signaling pathways. *Biochim Biophys Acta* 1801:1239-1248, 2010

47. von Eckardstein,A, Sibler,RA: Possible contributions of lipoproteins and cholesterol to the pathogenesis of diabetes mellitus type 2. *Curr Opin Lipidol* 22:26-32, 2011

48. Engin,F, Hotamisligil,GS: Restoring endoplasmic reticulum function by chemical chaperones: an emerging therapeutic approach for metabolic diseases. *Diabetes Obes Metab* 12 Suppl 2:108-115, 2010

49. Lilla,V, Webb,G, Rickenbach,K, Maturana,A, Steiner,DF, Halban,PA, Irminger,JC: Differential gene expression in well-regulated and dysregulated pancreatic beta-cell (MIN6) sublines. *Endocrinology* 144:1368-1379, 2003

Figure Legends

Figure 1. **HDLs protect beta cells against apoptosis induced by ER stress**

A. Human islets from cadaveric donors were dissociated using trypsin and plated. The next day, islets were treated or not with 10 µM TG in the presence or in the absence of HDLs for 24 hours. Cells were then fixed and apoptosis was assessed by scoring pycnotic nucleus. **B.** Cultured rat islets were incubated 24 hours in serum free-RPMI containing 5 g/l BSA and 10 mM glucose with the indicated combinations of 1 µM TG and 1 mM HDL. Cell death was determined by TUNEL in insulin-expressing cells on histological sections of the islets. Results are expressed as the percentage of apoptotic cells among insulin-positive cells in a given islet section. A minimum of 2'000 cells from at least 20 islets have been scored from two independent experiments. **C.** MIN6 were treated with 0.5 µM TG in the presence or in the absence of 1 mM HDL for 24 h. Cells were then fixed, and apoptosis was determined. Alternatively, the cells were lysed and the extent of caspase-3 activation was assessed by Western blotting using an antibody recognizing the cleaved active form of the protease. An actin-specific antibody was also used on the same blot to assess the evenness of loading. **D.** MIN6 cells were left untreated (Ctrl) or treated for 48 hours with 0.3% BSA (BSA) or 0.3% BSA/0.4 mM palmitate (P) in the presence or in the absence of 1 mM HDLs. Apoptosis was then scored as in panel A. **E-F.** Cultured rat islets were incubated for a week in serum-free RPMI medium containing 5 g/l BSA and 10 or 30 mM glucose (labeled G10 and G30 in the figure) in the presence (HDL) or in the absence (VEH) of 1 mM HDLs. Apoptosis was then assessed as in panel B. Panel E shows representative examples of TUNEL staining (green staining) in insulin-positive cells (red staining; nuclei are stained in blue with DAPI). The corresponding quantitation is shown in panel F.

Figure 2. **HDLs inhibit the induction of stress markers by TG and palmitate**

MIN6 cells and rat islets were left untreated (C) or treated with 0.5 µM TG during 6 hours (panels A-C and E) or 24 hours (panels D and F) in the presence or in the absence of 1 mM HDLs. Alternatively, the cells were treated with 0.3% BSA (BSA) or with 0.3% BSA/0.4 mM palmitate (P) in the presence or in the absence of 1 mM HDLs for 24 hours (panel A, B) or 48 hours (panel C). The cells were then lysed and RNA and proteins were isolated. The extent of XBP1 mRNA splicing was then determined

(panel A). The pound sign indicates an unspecific band (see the methods). CHOP mRNA expression was determined by quantitative PCR (panel B). Western blot analysis were performed to assess protein expression of CHOP (panel C), BiP (panel D), phospho-PERK (panel E), and phospho- and total JNK (F). The experiments presented in panels E and F were repeated once and twice, respectively, and yielded similar results.

Figure 3. **HDLs prevent TG- and palmitate-induced ER morphology alterations**

MIN6 cells were plated on glass slide previously coated with poly-L-lysine and incubated for 6 hours with the indicated treatments (panel **A**). Alternatively, the cells were treated for 6 hours with TG and then incubated or not with HDLs for an additional 18 hour-period (panel **B**). In panel C; the cells were incubated for 12 hours with 0.3% BSA, 0.4 mM palmitate, and 1 mM HDLs in the indicated combinations. The cells were then processed for EM as described in the methods.

Figure 4. **Insulin overexpression-induced beta cell apoptosis is inhibited by HDLs**

MIN6 cells were infected with lentiviruses encoding the indicated constructs. Three days later, cells were trypsinized and plated in new culture dishes for 4 days, the last two days in the presence or in the absence of 1 mM HDLs. Apoptosis was then determined by scoring pycnotic and fragmented nuclei (panel **A**). Alternatively, 24 hours after the infection, the extent of XBP1 mRNA splicing (panel **B**) and CHOP mRNA expression (panel **C**) were determined.

Figure 5. **HDL-mediated beta cell protection against TG-induced apoptosis is inhibited by BFA**

A-B. MIN6 cells were infected with VSVG-GFP-encoding lentiviruses and treated two days later with or without 0.5 µM TG in the presence or in the absence of 1 mM HDLs for 5 hours at 40°C. The cells were then incubated or not for an additional 1 hour time period at 32°C. The presence of folded VSVG was assessed by immuno-cytochemistry on permeabilized cells using an antibody specifically recognizing the correctly folded form of the protein. The percentage of cells expressing folded VSVG was quantitated and shown in panel B. **C-E**. Cells were treated as in panel A except that non-

permeabilized cells were labeled with an antibody directed against the ectopic part of VSVG. The percentage of cells expressing VSVG at the cell surface was quantitated and shown in panel D. Quantification of the GFP fluorescence intensity in VSVG-GFP expressing cells is presented in panel E. **F-G**. MIN6 cells infected with VSVG-GFP-encoding lentiviruses cells were pre-incubated or not with 250 ng/ml BFA for 2 hours before being subjected to the indicated combinations of 0.5 μM TG and 1 mM HDLs for an additional 22 hour-period. Permeabilized cells were then stained with an antibody recognizing GM130, a specific Golgi marker (panel **F**). Alternatively, apoptosis was assessed by scoring cells with pycnotic and/or fragmented nucleus (panel **G**). Means with different symbol (# or &) are significantly different. Nuclei were stained in blue with the Hoechst 33342 dye.

Figure 6: **HDLs restore ER to Golgi trafficking in palmitate-treated cells**

MIN6 cells were infected with VSVG-GFP-encoding lentiviruses and treated or no with 0.4 mM palmitate in the presence or in the absence of 1 mM HDLs for 48 hours (in each case, BSA was present at a 0.3% concentration). The cells were then incubated 5 hours at 40°C. They were then treated for 15 minutes with 5 μM cycloheximide before switching the temperature to 32°C for 0 or 30 minutes (note that the temperature shifts and/or cycloheximide did not induce apoptosis; see Supplemental Figure 8). The cells were stained with an antibody recognizing the Golgi marker GM130 (red staining; left part of panel **A**) or processed as described in Figure 5A-B (right part of panel **A**). Nuclei were stained in blue with the Hoechst 33342 dye. Representative examples of the different locations of VSVG in cells are shown in panel **B** (VSVG mainly in the ER when the GFP signal does not colocalize with GM130 staining; VSVG mainly in the Golgi when these two signals extensively colocalize; and intermediate situation when the GFP signal only partially colocalizes with the Golgi marker). Panel **C** depicts the quantitation of the percentage of cells with VSVG mainly localized in the Golgi and panel **D** the quantitation of the percentage of cells with correctly folded VSVG (results derived from 5 independent experiments each). Ctrl, control.

Figure 7: **Oxidized HDLs do not protect beta cells against TG-induced apoptosis**

MIN6 cells were treated with 0.5 μM TG in the presence or in the absence of 1 mM non-oxidized or oxidized HDLs (oxidation performed during 8 hours or 16 hours) for 24 hours. Cells were then fixed and apoptosis was assessed by scoring pycnotic nuclei.

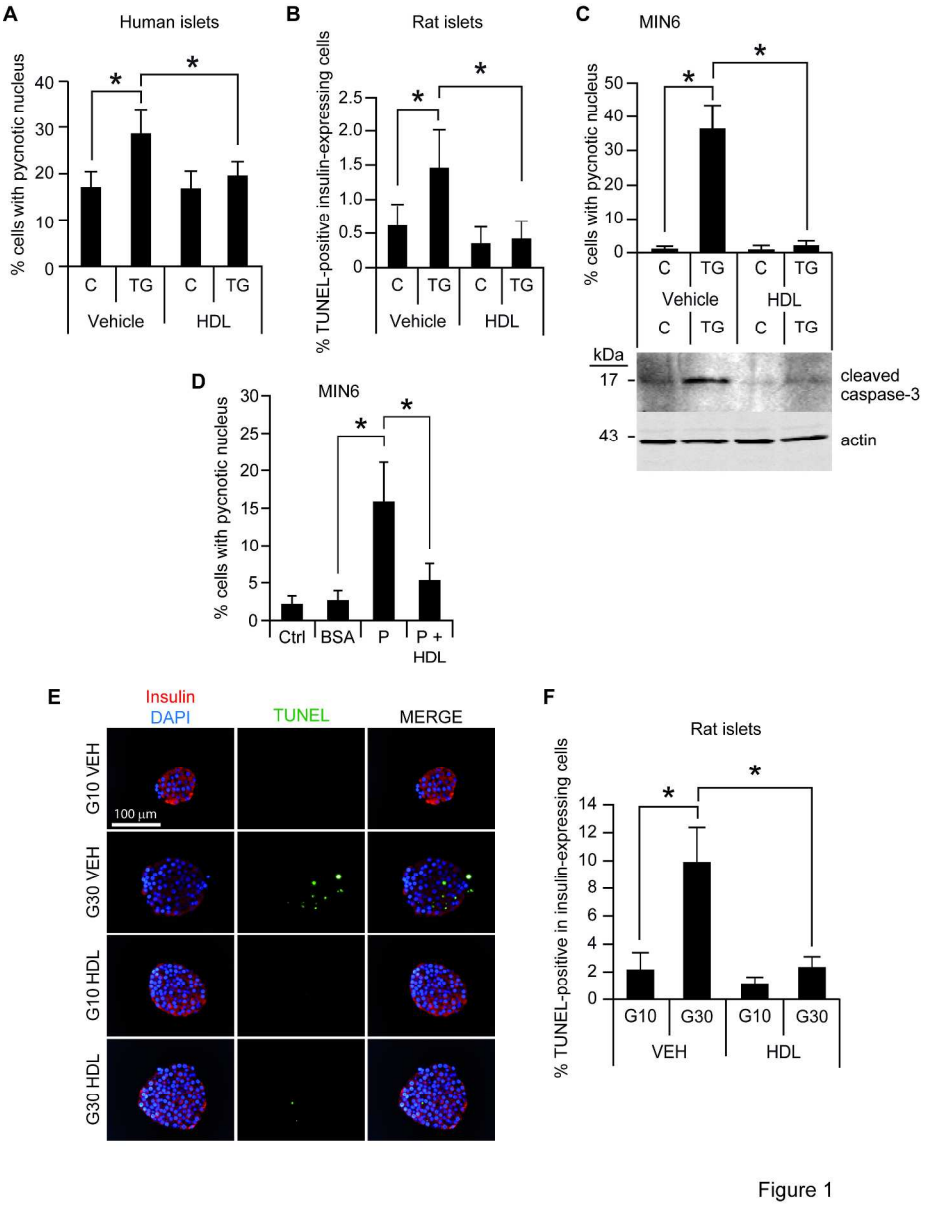

Figure 1

245x321mm (300 x 300 DPI)

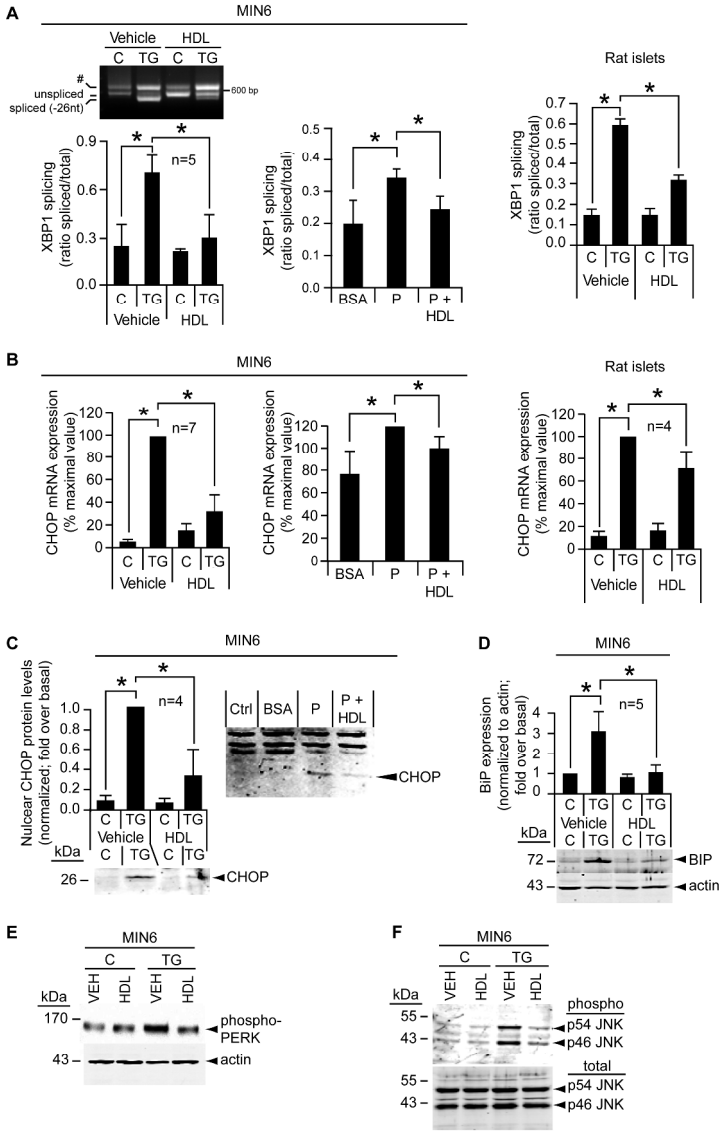

Figure 2

289x487mm (300 x 300 DPI)

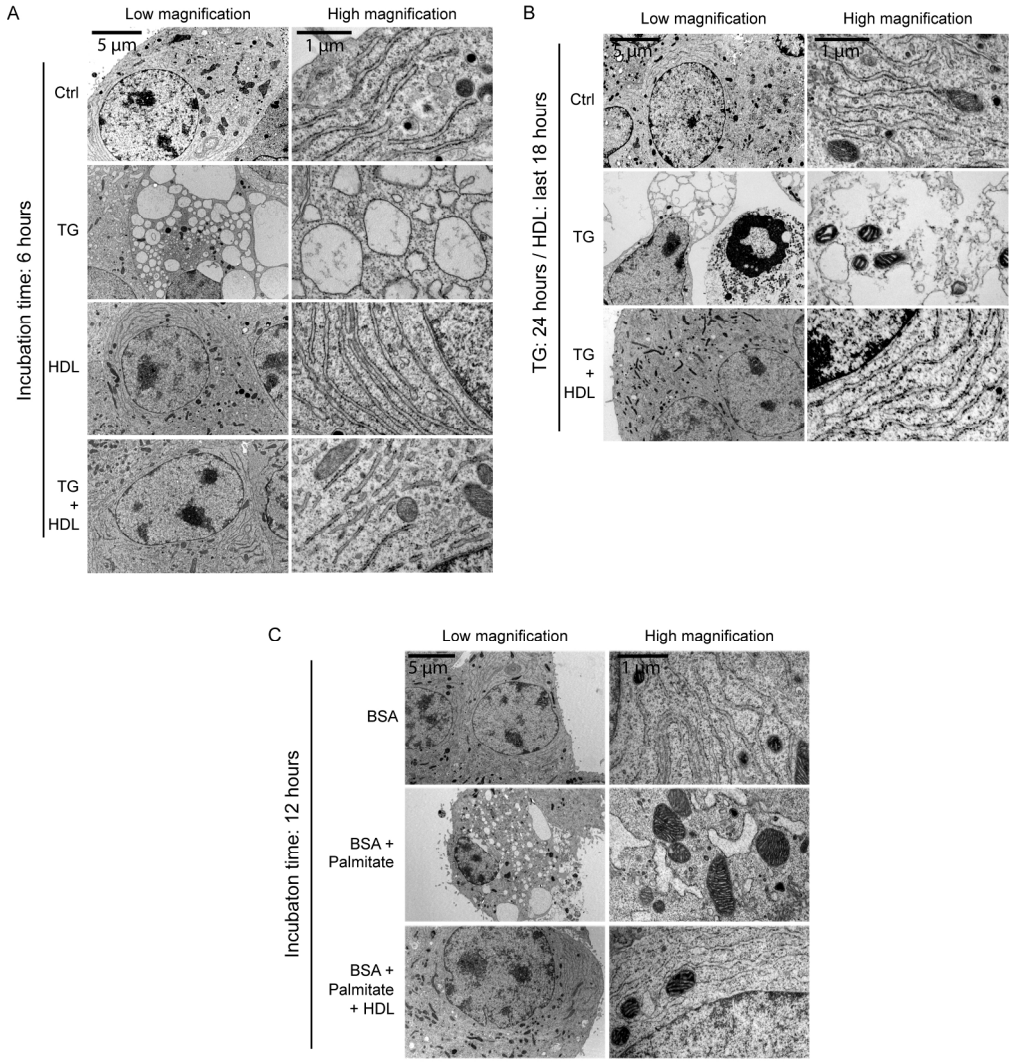

Figure 3

236x276mm (300 x 300 DPI)

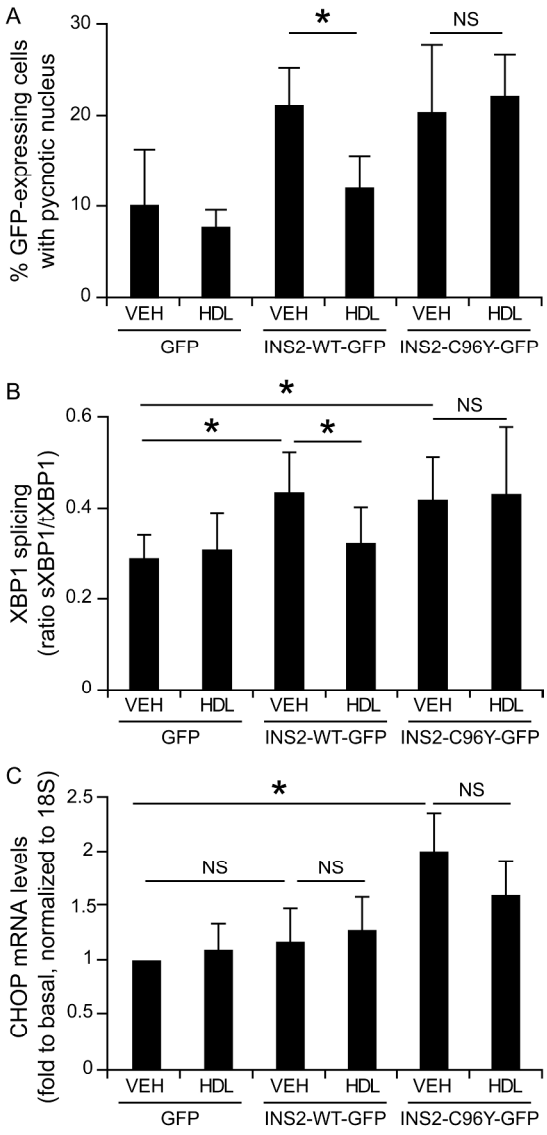

Figure 4

223x496mm (300 x 300 DPI)

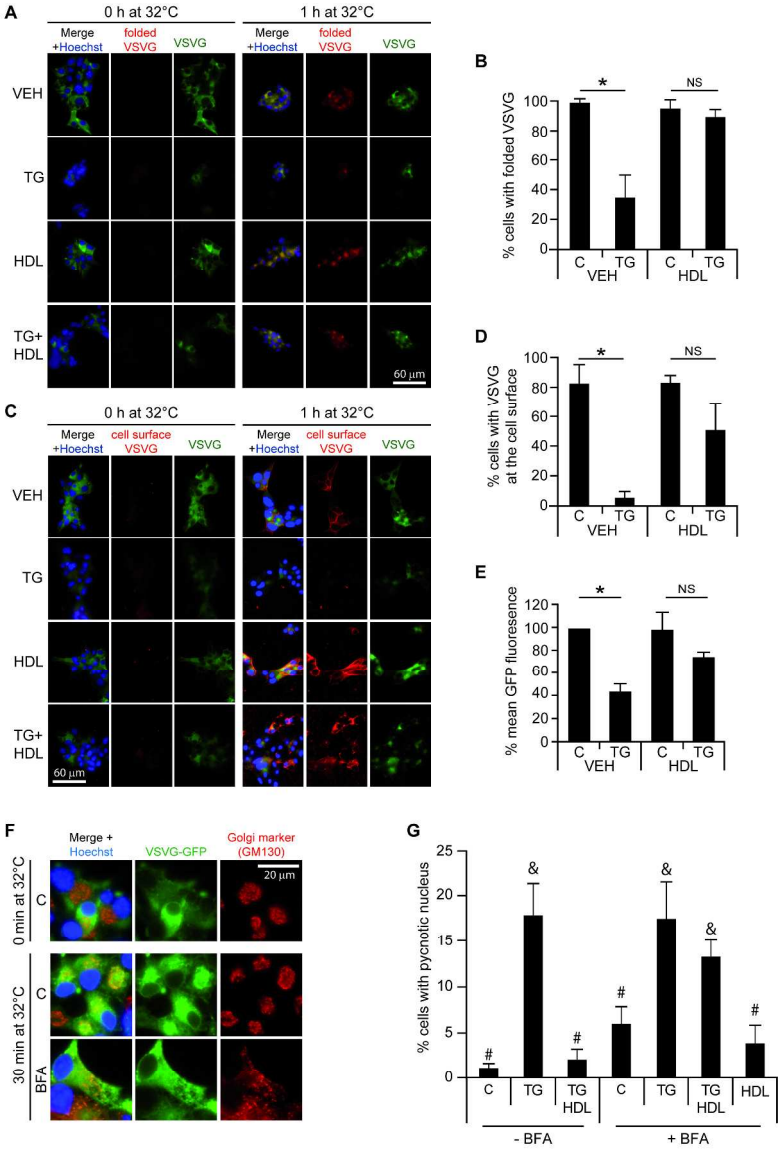

Figure 5

286x441mm (300 x 300 DPI)

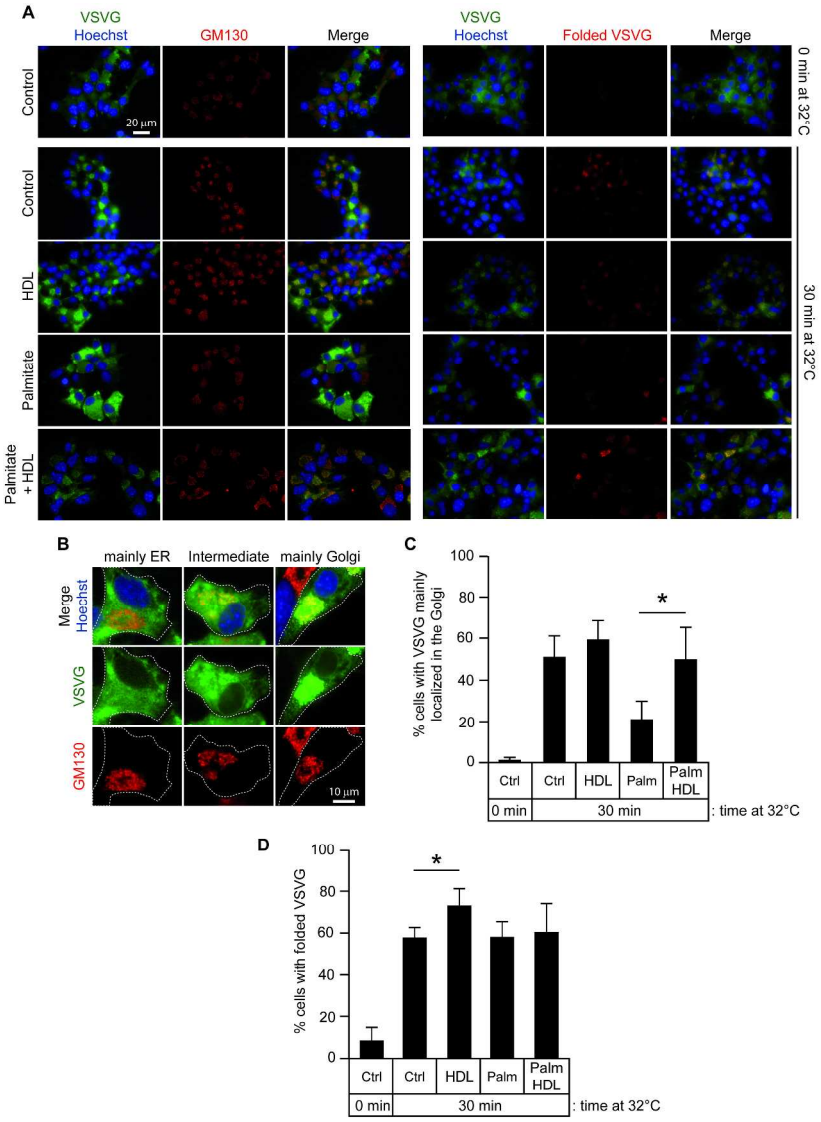

Figure 6

290x409mm (300 x 300 DPI)

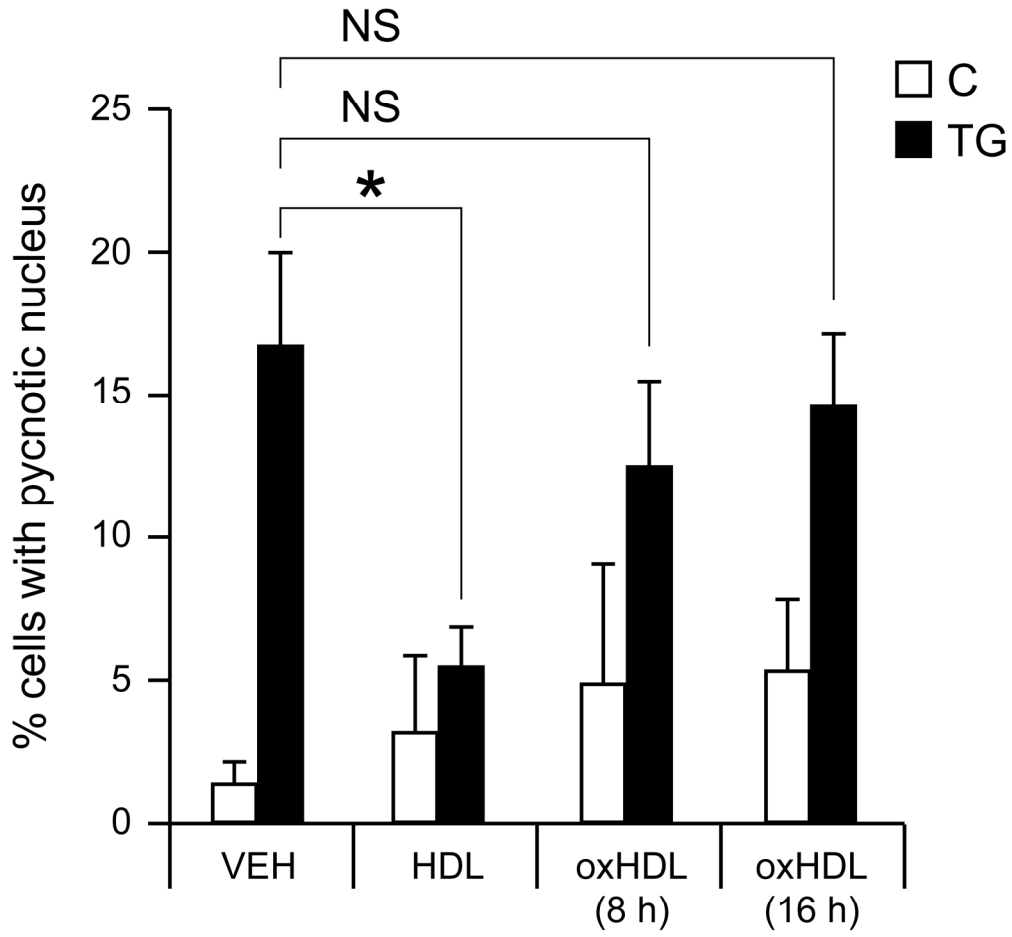

Figure 7

105x115mm (600 x 600 DPI)

Supplemental Table 1 : **Human islet quality and clinical characteristics of the donors**

Donor	Age (years)	Gender	Cause of Death	Islet cell viability	Islet purity
1	38	Female	Cerebral ischemia	90%	75%
2	57	Female	Vascular complication	90%	60%
3	52	Female	Cerebral hemorrhage	85%	89%
4	48	Male	Cerebral bleeding	90%	70%

Supplemental Table 2: **Quantitation of insulin in MIN6 infected with lentiviruses encoding GFP, INS2-WT-GFP and INS2-C96Y-GFP**. Enzyme immune assay was performed to quantitate the amount of insulin in MIN6 cells in the different conditions used in Figure 4. Insulin content was measured using the rat insulin EIA kit from SpiBio (Basel, Switzerland; catalog n°A05105) according to the manufacturer's instructions. Results correspond to the mean ± SD (n=3).

	Insulin enzyme-immuno-assay	
	fmoles insulin per cell	fold
Control (GFP)	0.30 ± 0.12	1.0
INS2-WT-GFP	0.46 ± 0.17	1.6 ± 0.1
INS2-C96Y-GFP	0.36 ± 0.12	1.2 ± 0.1

MIN6 cells were cultured at 25 mM glucose. In this condition, the biosynthetic production of insulin is likely maximal in these cells and was calculated earlier to be about one femtomole per cell (1). Here, quantitation of insulin in MIN6 cells cultured at 25 mM glucose gave a value of 0.3 femtomoles of insulin per cell. In wild-type insulin-overexpressing cells, the insulin content increased by 60 %. Apparently therefore, infection with INS-WT-GFP-encoding lentiviruses was able to increase biosynthesis of insulin in Min6 cells and this correlated with the induction of XBP1 splicing (see Figure 4B). It is relevant to note that the insulin-GFP fusion protein is targeted appropriately to insulin granules (2). The calculated increase of insulin content in mutant insulin-overexpressing cells was lower but this likely reflects the fact that anti-insulin antibodies may not recognize this mutant form (3).

1. Ishihara,H, Asano,T, Tsukuda,K, Katagiri,H, Inukai,K, Anai,M, Kikuchi,M, Yazaki,Y, Miyazaki,JI, Oka,Y: Pancreatic beta cell line MIN6 exhibits characteristics of glucose metabolism and glucose-stimulated insulin secretion similar to those of normal islets. Diabetologia 36:1139-1145, 1993

2. Ohara-Imaizumi,M, Nakamichi,Y, Tanaka,T, Ishida,H, Nagamatsu,S: Imaging exocytosis of single insulin secretory granules with evanescent wave microscopy: distinct behavior of granule motion in biphasic insulin release. J Biol Chem 277:3805-3808, 2002

3. Wang,J, Takeuchi,T, Tanaka,S, Kubo,SK, Kayo,T, Lu,D, Takata,K, Koizumi,A, Izumi,T: A mutation in the insulin 2 gene induces diabetes with severe pancreatic beta-cell dysfunction in the Mody mouse. J Clin Invest 103:27-37, 1999

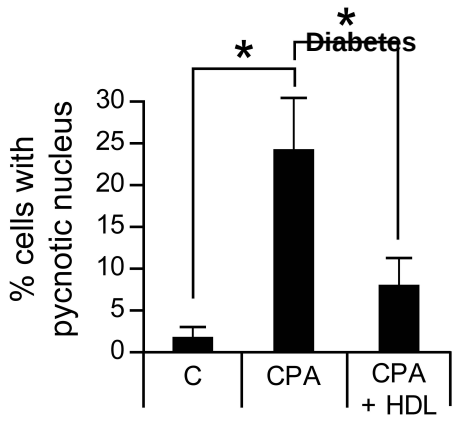

Supplemental Figure 1. **HDLs protect MIN6 cells against apoptosis induced by CPA** MIN6 cells were treated with 100 μM CPA in the presence or in the absence of 1 mM HDLs for 24 hours. Cells were then fixed, and apoptosis was determined as in Figure 1C.

A

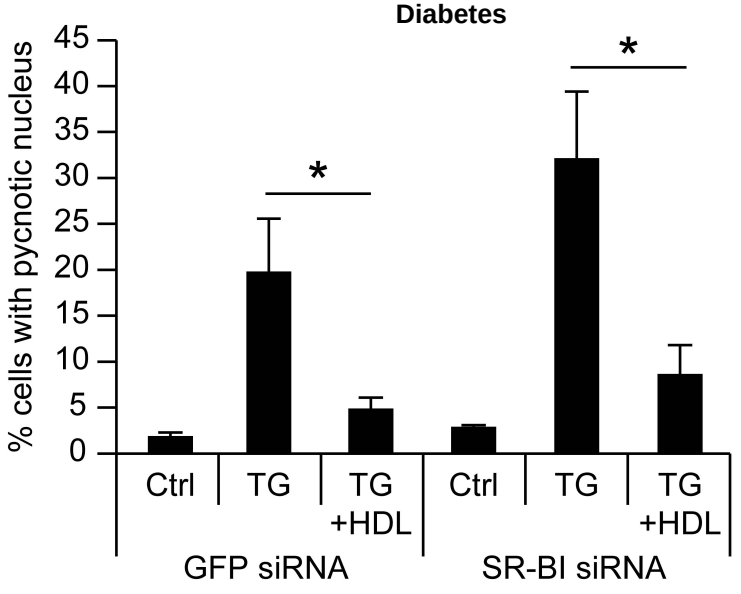

B

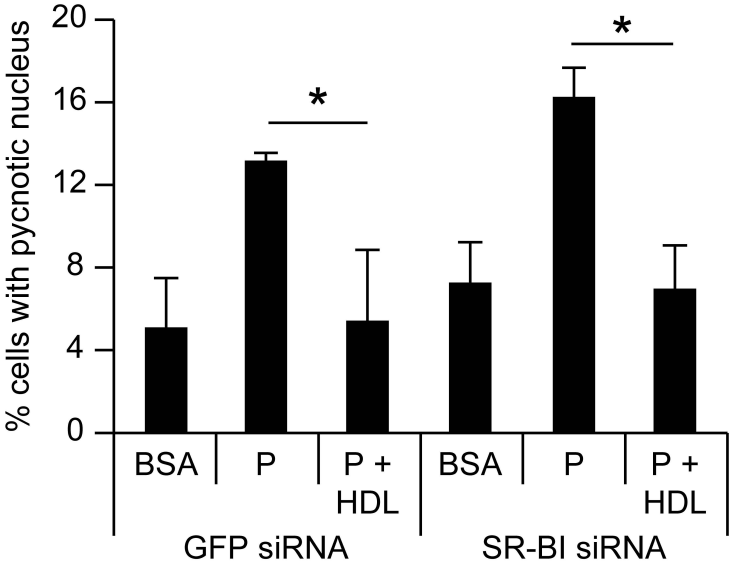

C

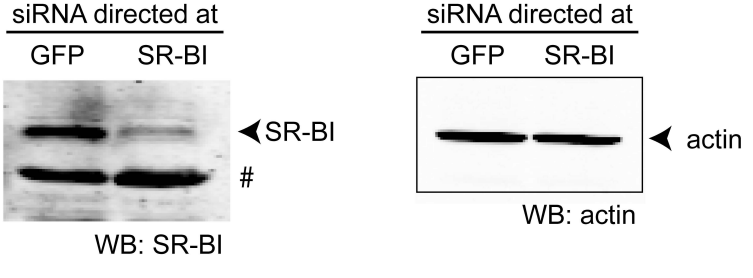

Supplemental Figure 2: **SR-BI does not mediate HDL protection against ER stress**
MIN6 cells were transfected with 300 pmoles of the indicated siRNAs and incubated for 2 days. The cells were then left untreated (Ctrl) or stimulated with 0.5 μM TG in the presence or in the absence of 1 mM HDLs for an additional 24 hour period (panel A). Alternatively, the cells were incubated 48 more hours with 0.3% BSA (the final concentration of BSA found in the palmitate condition) or 0.4 mM palmitate (P), again in the presence or in the absence of 1 mM HDLs (panel B). Apoptosis was then assessed. Panel C shows the expression of SR-BI and actin as assessed by Western blot analysis three days after the addition of the siRNAs. #, non-specific band.

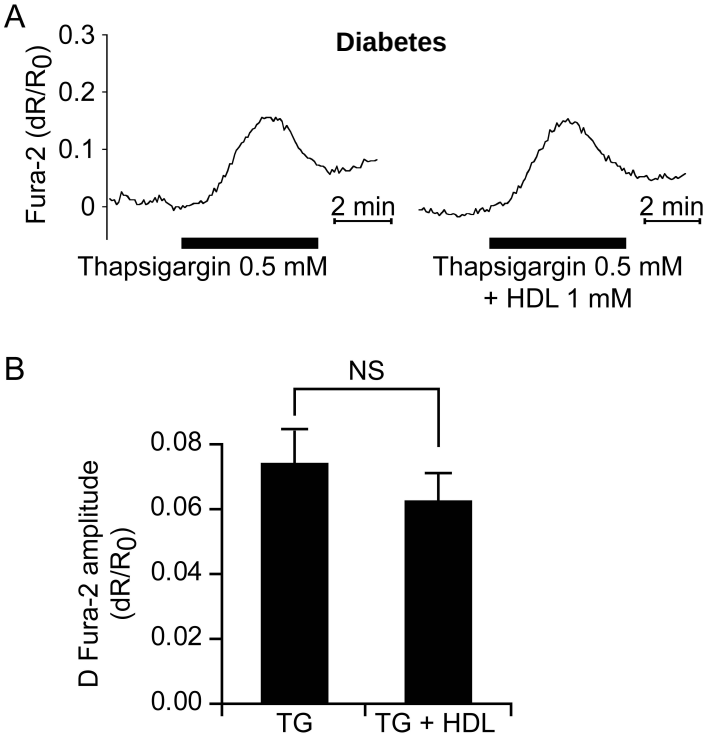

Supplemental Figure 3. **HDLs do not inhibit TG-induced cytosolic calcium increase**

A. Representative traces of cytosolic free Ca^{2+} released from intracellular stores following the addition on MIN6 cells of 0.5 µM thapsigargin, pre-incubated or not for 12 minutes with 1 mM HDLs. Values on the y axis correspond to the variation over time in the 340 nm over 380 nm Fura-2 fluorescence excitation ratio (D R/R0; where R0 is the initial fluorescence ratio recorded at the beginning of the experiment). B. Comparison of store-released Ca^{2+} in the presence or the absence of 1 mM HDL. Results are expressed as maximum amplitude of Fura-2 ratio changes induced by 0.5 µM thapsigargin application. Data are means ± 95%CI of 24 cells (control) and 33 cells (HDL) from 3 (control) and 4 (HDL) independent experiments.

Method associated with this figure: Fluorescence calcium imaging

Intracellular calcium was measured using Fura-2 (Teflabs, Austin, TX, USA) loaded into cells by incubation with 8 µM Fura-2 AM for 45 min at 37°C in a HEPES-buffered balanced solution containing (mM): NaCl 160, KCl 5.4, HEPES 20, $CaCl_2$ 1.3, $MgSO_4$ 0.8, NaH_2PO_4 0.78, glucose 20 and that was supplemented with 0.1 % Pluronic F-127 (Molecular Probes, Eugene, OR). Once loaded with dye, cells were placed in a perfusion chamber designed for rapid exchange of perfusion solutions (1). Experiments were performed in an experimental solution containing (mM): NaCl 160, KCl 5.4, $CaCl_2$ 1.3, $MgSO_4$ 0.8, NaH_2PO_4 0.78, HEPES 20, glucose 5, pH 7.4, bubbled with air. Experiments were carried out on the stage of an inverted epifluorescence microscope (Carl Zeiss, Jena) and observed through a 40x 1.3 N.A. oil-immersion Neofluar objective lens (Zeiss).

(1) Chatton,JY, Marquet,P, Magistretti,PJ: A quantitative analysis of L-glutamate-regulated Na^+ dynamics in mouse cortical astrocytes: implications for cellular bioenergetics. Eur J Neurosci 12:3843-3853, 2000.

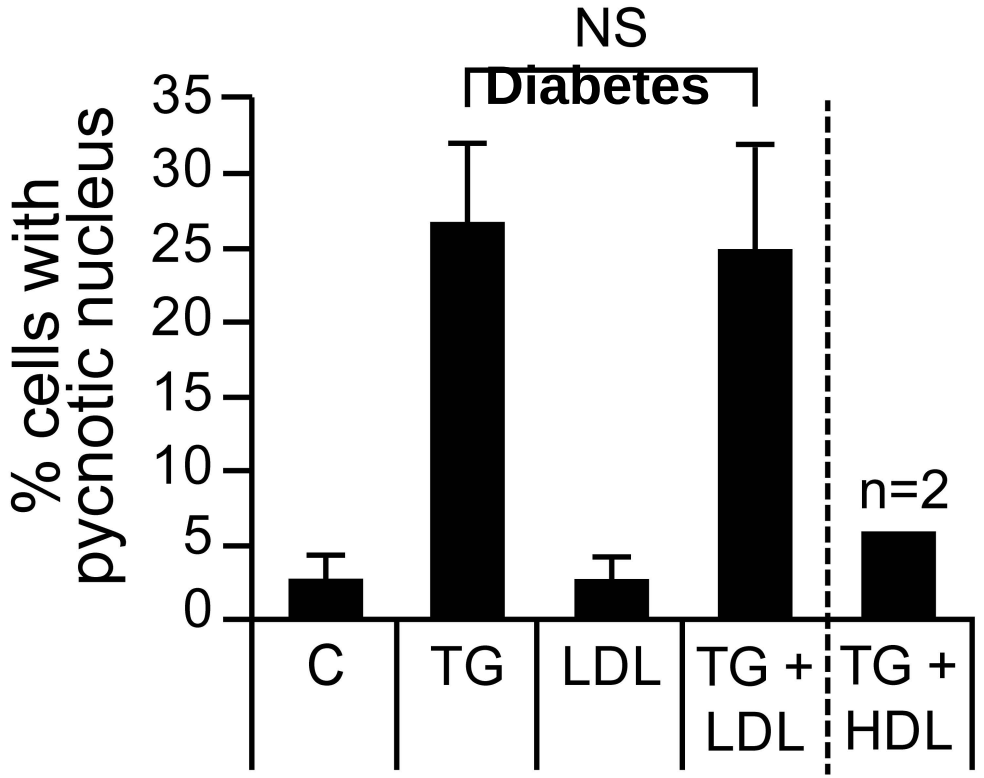

Supplemental Figure 4. **LDLs do not inhibit TG-induced apoptosis** MIN6 cells were treated with 0.5 µM TG in the presence or in the absence of 1 mM native LDL for 24 hours. Cells were then fixed, and apoptosis was determined by scoring the percentage of cells displaying pycnotic nucleus. As a control, TG was also incubated with 1 mM HDLs (bar on the right side of the dashed line). This led, similarly to what was shown in Figure 1, to efficient inhibition of apoptosis.

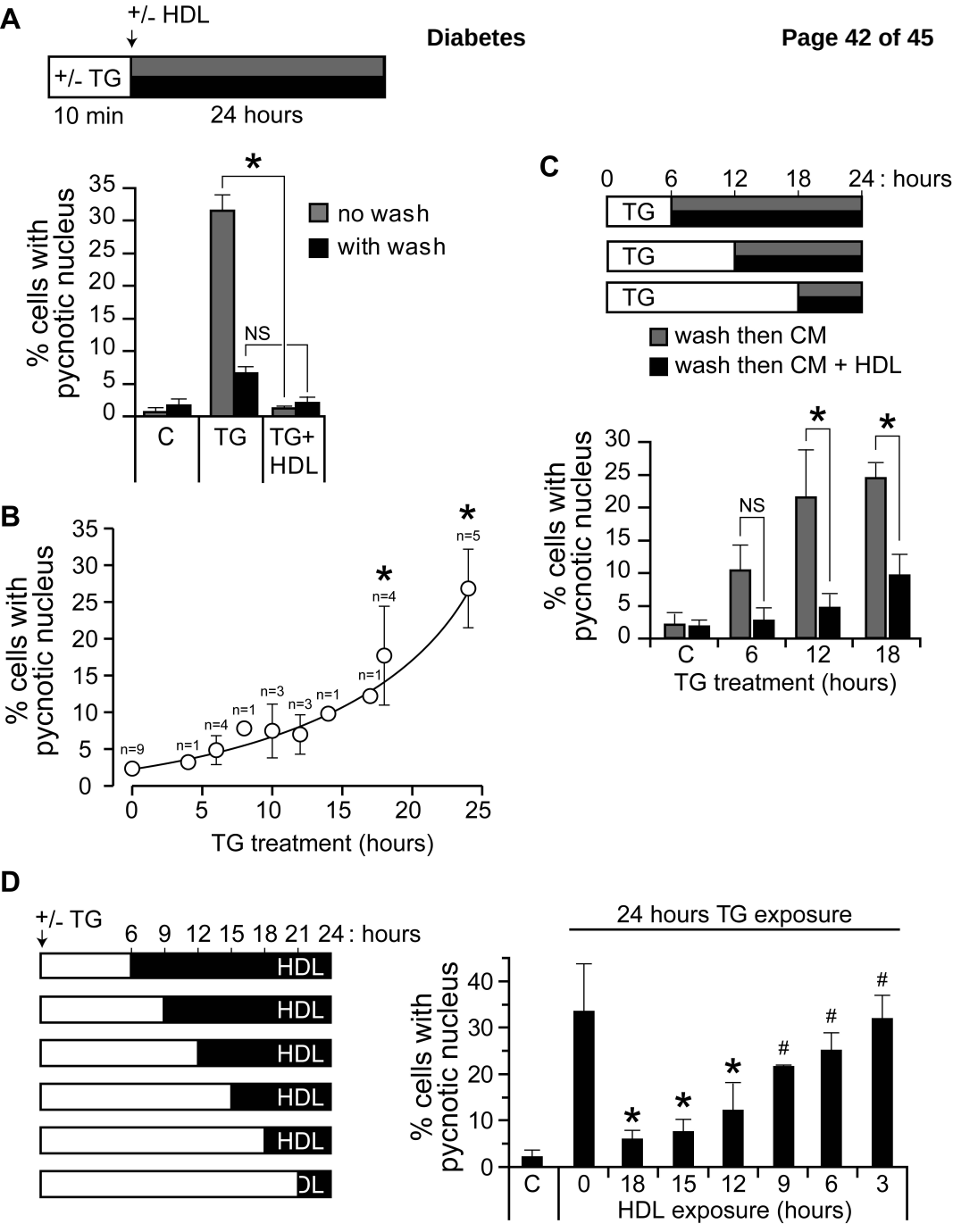

Supplemental Figure 5. **Kinetics of HDL and TG effects on MIN6 cells** **A**. MIN6 cells were treated with 0.5 µM TG for 10 minutes. The cells were then washed or not, and stimulated with 1 mM HDL for 24 hours or left untreated. Cells were then fixed, and apoptosis was determined. **B**. MIN6 cells were treated with 0.5 µM TG for the indicated periods of time and fixed for apoptosis counting. **C**. MIN6 cells were treated for the indicated periods of time with 0.5 µM TG. The medium was then removed and fresh culture medium (CM) was added containing or not 1 mM HDLs. The cells were fixed 24 hours after the beginning of the experiments and apoptosis was determined. **D**. MIN6 cells were treated with 0.5 µM TG for the indicated periods of time. One mM HDL was then added to the culture medium (no wash). Cells were fixed 24 hours after the beginning of the experiments and apoptosis was scored.

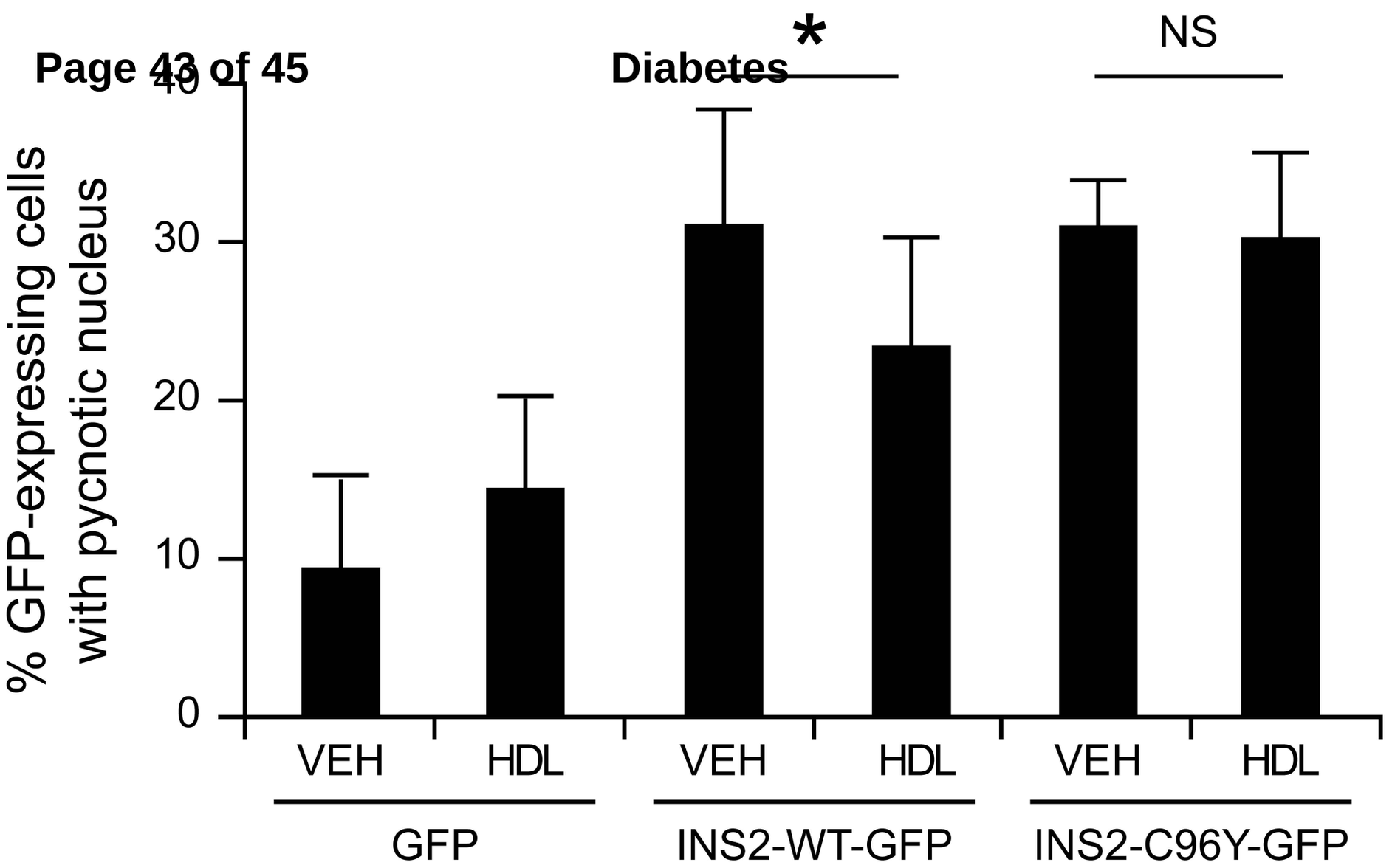

Supplemental Figure 6. **HDLs protect MIN6 cells from apoptosis induced by transfection of wild-type insulin but not of the C96Y insulin mutant**

MIN6 cells were transfected with the plasmids encoding the indicated constructs. The following day, cells were incubated or not with 1 mM HDL for 48 hours. Apoptosis was then determined by scoring pycnotic and fragmented nuclei. The results are derived from 4 independent experiments.

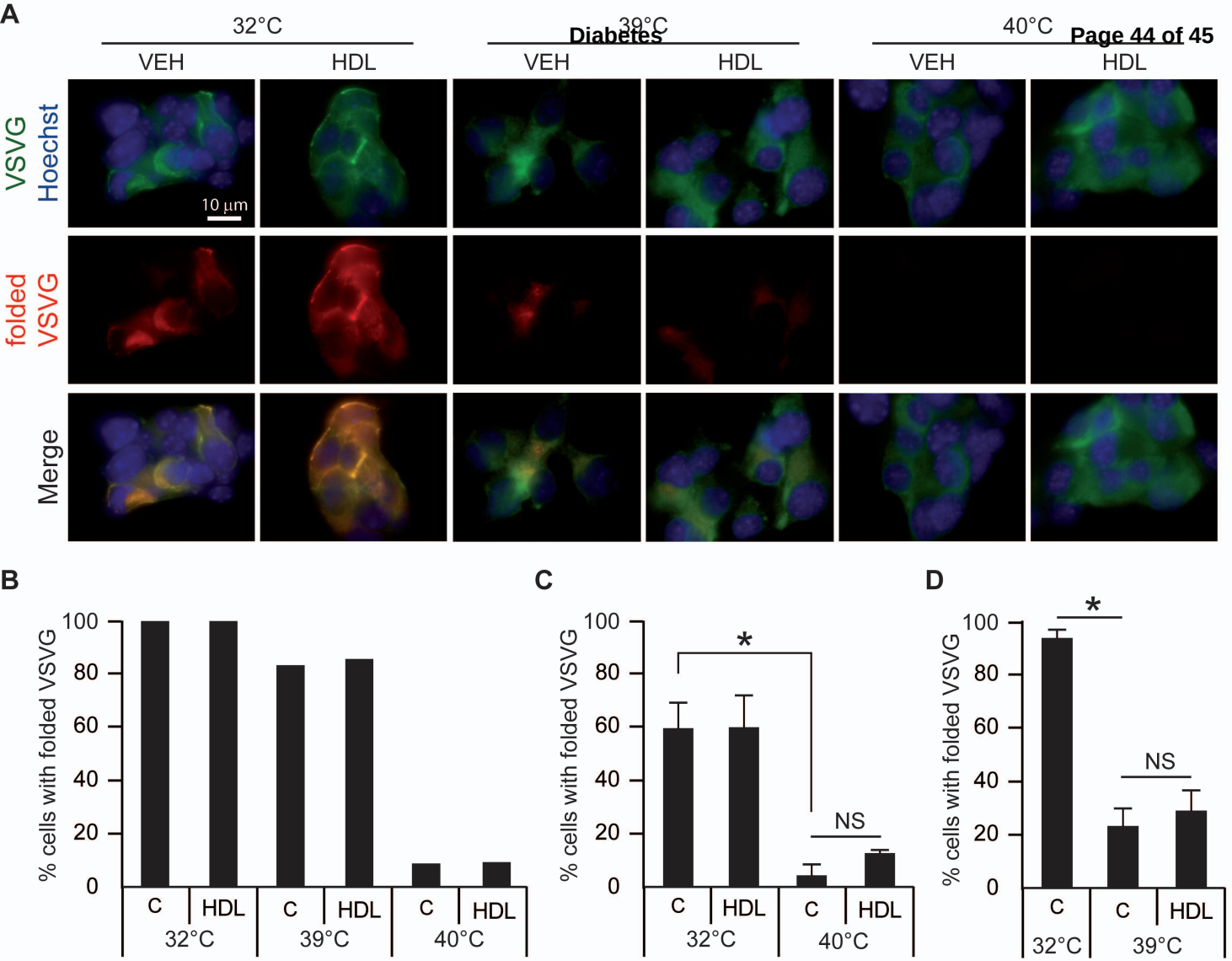

Supplemental figure 7: **HDLs do not prevent heat-induced VSVG misfolding**
A-B. MIN6 cells were infected with VSVG-GFP-encoding lentiviruses for 48 hours and then treated with HDL or vehicle and further incubated at the indicated temperatures for 24 hours. Cells were then fixed and stained with Hoechst 33342 (blue staining). Immunocytochemistry against the native form of VSVG was then performed (red staining). VSVG-GFP, whether correctly folded or not, corresponds to the green staining. Quantitation of the percentage of green cells expressing a correctly folded VSVG is shown in panel B. **C-D**. MIN6 cells were transfected with 4 µg of a VSVG-GFP-encoding vector and then treated as in panel A-B. The results presented in panel C are derived from 5 independent experiments.

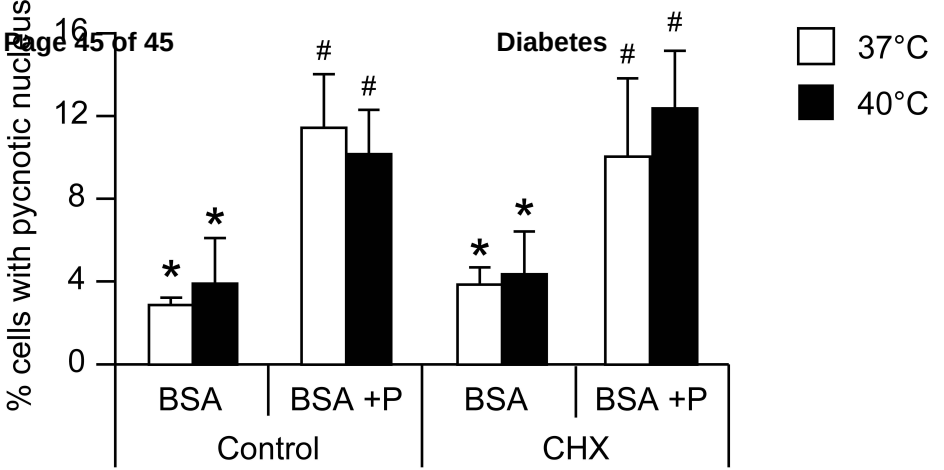

Supplemental Figure 8: **Cycloheximide and temperature shifts do not affect beta cell survival**

MIN6 cells were subjected to the same treatment as described in Figure 6 before apoptosis was assessed. Namely, cells were incubated 48 hours with 0.3% BSA (BSA) or 0.3% BSA/0.4 mM palmitate (BSA + P). The cells were then maintained at 37°C or switched to 40°C for 5 hours. The last 15 minutes, the cells were incubated or not with 5 µM cycloheximide (CHX). Cells were finally incubated at 32°C for an additionnal 30 minute period before being fixed and scored for the presence of pycnotic nucleus. Conditions with the same symbol (* or #) are not significantly different.